Supporting Information for "Improved Parameterizations of Vertical Ice-Ocean Interfaces"

Ken X. Zhao[1], Eric D. Skyllingstad[1], and Jonathan D. Nash[1]

[1]College of Earth, Ocean, and Atmospheric Sciences, Oregon State University, 2651 SW Orchard Ave., Corvallis, OR 97331-5503.

Contents of this file

S-1. Wall-Bounded Plume Theory

S-1.1. General Equations for Mass, Momentum, and Buoyancy

The basic formulae for an entraining point or line source plume (representing a discharge plume) and a sheet plume (representing a distributed melt plume) along a wall are revisited in this subsection.

We start with the Boussinesq mass, vertical momentum, and buoyancy equations

$$\frac{\partial u}{\partial x} + \frac{\partial v}{\partial y} + \frac{\partial w}{\partial z} = 0\,, \tag{1a}$$

$$\frac{\partial w}{\partial t} + u\frac{\partial w}{\partial x} + v\frac{\partial w}{\partial y} + w\frac{\partial w}{\partial z} = -\frac{1}{\rho_a}\frac{\partial p}{\partial z} + b + \nu\nabla^2 w\,, \tag{1b}$$

August 8, 2023, 6:47am

:

$$\frac{\partial b}{\partial t} + u\frac{\partial b}{\partial x} + v\frac{\partial b}{\partial y} + w\frac{\partial b}{\partial z} = \kappa \nabla^2 b \,, \tag{1c}$$

where $\nu = 1.8 \times 10^{-6}$ m^2/s is the molecular kinematic viscosity and $\kappa \approx \kappa_S = 7.2 \times 10^{-10}$ m^2/s is the molecular scalar diffusivity responsible for buoyancy, which is dominated by salinity near an ice-ocean boundary layer. Here, the vertical velocity $w(x, z, t)$ is in the z-direction along the wall and plume, the horizontal velocity $u(x, z, t)$ is in the x-direction normal to the wall and plume, and the wall is defined to be at $x = 0$. The deviation from hydrostatic pressure is $p(x, z, t)$ and the buoyancy is $b(x, z, t) = g(\rho_a(z) - \rho(x, z, t))/\rho_a$, where ρ is the density of the plume and $\rho_a(z)$ is the far-field density of the ambient fluid. Here, the Boussinesq approximation assumes that $\rho_a - \rho \ll \rho_a$.

We can then decompose the terms in this equation into time-averaged and eddy components for $w(x, z, t) = \overline{w}(x, z) + w'(x, z, t)$ and similarly for the other time-dependent variables. We may also assume that all quantities are independent of the horizontal y-direction so that all ∂_y terms vanish. Assuming a psuedo-steady state with no time-mean tendency terms, the time-mean mass, momentum, and buoyancy equations are

$$\frac{\partial \overline{u}}{\partial x} + \frac{\partial \overline{w}}{\partial z} = 0 \,, \tag{2a}$$

$$\overline{u}\frac{\partial \overline{w}}{\partial x} + \overline{w}\frac{\partial \overline{w}}{\partial z} + \frac{\partial \overline{w'^2}}{\partial z} + \frac{\partial \overline{u'w'}}{\partial x} = -\frac{1}{\rho_a}\frac{\partial \overline{p}}{\partial z} + \overline{b} + \nu\frac{\partial^2 \overline{w}}{\partial x^2} \,, \tag{2b}$$

$$\overline{u}\frac{\partial \overline{b}}{\partial x} + \overline{w}\frac{\partial \overline{b}}{\partial z} + \frac{\partial \overline{u'b'}}{\partial x} + \frac{\partial \overline{w'b'}}{\partial z} = \kappa\frac{\partial^2 \overline{b}}{\partial x^2} \,, \tag{2c}$$

Next, we add boundary conditions to the 2D time-averaged mass, momentum, and buoyancy equations that are appropriate for the wall-bounded plume problem at the wall, the quiescent far-field, and the wall fluxes,

$$\overline{w}(0, z) = \overline{u'w'}(0, z) = \overline{u'b'}(0, z) = 0 \,, \tag{3a}$$

$$\overline{w}(\infty, z) = \overline{u'w'}(\infty, z) = \overline{u'b'}(\infty, z) = 0 \,, \tag{3b}$$

$$\overline{u}(0, z) = m, \ \left.\frac{\partial \overline{b}}{\partial x}\right|_{x=0} = \frac{mB}{\kappa} \,, \tag{3c}$$

where $m(z)$ is the wall-source volume flux per unit area (i.e., the sum from melting and subglacial discharge) and mB is the additional wall-source buoyancy flux per unit length for a buoyancy anomaly B.

At the stage, Eqs. (2a)-(3c) fully describe the wall-bounded plume system with a wall source of buoyancy flux. Within the laminar boundary layer (less than a millimeter in the ice-ocean boundary layer), the time time-varying terms are small and we can derive analytical solutions (see Wells and Worster (2008)) for $w(x, z)$, $u(x, z)$ and $b(x, z)$. This is briefly discussed in the next section (on ice-ocean boundary layers). However, in general it is important to understand the profiles of w,u, and b outside of the laminar boundary layers where the eddy covariance terms are comparable and or larger than the molecular viscosity terms (e.g., $\partial_x \overline{u'b'} \geq \kappa \partial_{xx} \overline{b}$ for the buoyancy equation). These eddy covariance terms may then be approximated as eddy viscosity and diffusion terms modeled by appropriate coefficients $\nu_e(x, z), \kappa_e(x, z)$, but currently there are only empirical functions for these functions based on laboratory experiments and DNS of the turbulent boundary layer (e.g., Gayen et al., (2016), Parker et al., (2020), Parker et al., (2021), and many others) rather than closed-form solutions. These empirical functions describe the x-direction variation of w,u, and b, which are further discussed in the next section. However, so far these experiments have mostly been limited to scales of meters and idealized environments rather than geophysical settings and scales. A turbulence closure model for eddy covariance terms at and ice-ocean interface was recently undertaken in Jenkins (2021),

August 8, 2023, 6:47am

and may prove fruitful in the future, but this approach requires observational testing and validation in geophysical contexts, particularly in the case of fast-melting and vertical ice-ocean interfaces.

S-1.2. Plume Theory

In this subsection, we derive the equations for the x-integrated mass, momentum, and buoyancy equations to solve for their z dependency. These equations form the basis for plume theory (see e.g., Morton, Taylor, and Turner (1956)).

To derive these equations, we first integrate Eqs. (2a)-(2c) w.r.t. x,

$$\frac{\partial}{\partial z}\underbrace{\int_0^\infty \overline{w}\,\mathrm{d}x}_{\equiv DW} = -\left.\overline{u}\right|_{x=0}^\infty , \tag{4a}$$

$$\frac{\partial}{\partial z}\underbrace{\int_0^\infty \frac{\overline{w}^2}{2}\,\mathrm{d}x}_{\equiv DW^2} + \left[\overline{u}\,\overline{w} + \overline{u'w'}\right]\big|_{x=0}^\infty = -\left(\frac{\partial}{\partial z}\int_0^\infty \overline{w'^2} + \frac{1}{\rho_a}\frac{\partial \overline{p}}{\partial z}\,\mathrm{d}x\right) + \underbrace{\int_0^\infty \overline{b}\,\mathrm{d}x}_{\equiv DB} + \nu\left.\frac{\partial \overline{w}}{\partial x}\right|_{x=0}^\infty , \tag{4b}$$

$$\frac{\partial}{\partial z}\underbrace{\int_0^\infty \overline{w}\overline{b} + \overline{w'b'}\,\mathrm{d}x}_{\equiv KDWB} + \left[\overline{u}\overline{b} + \overline{u'b'}\right]\big|_{x=0}^\infty = \kappa\left.\frac{\partial \overline{b}}{\partial x}\right|_{x=0}^\infty , \tag{4c}$$

where we can define a characteristic plume vertical velocity W, buoyancy B, and width D. Note that W is inconsistently defined in the literature, but here we define it as the horizontally-averaged vertical velocity at each depth.

Next we can make the following assumptions based on Morton et al. (1956). The entrainment of ambient fluid is proportional to the characteristic vertical velocity at each depth, $\overline{u}(\infty, z) = -\alpha W$. The first integral on the right hand side of Eq. (4b) is higher order and assumed to be small compared to the other terms. In addition, previous experiments have shown that K (from Eq. (4c) is a constant and is approximately equal to 1 (Parker et

al., 2021). We can also make the shear boundary layer approximation $\nu\,\partial_x \overline{w}|_{x=0} = C_d W^2$ with a skin friction coefficient C_d.

Substituting the boundary conditions from Eqs. (3a)-(3c),

$$\frac{\partial(DW)}{\partial z} = \alpha W + m\,, \tag{5a}$$

$$\frac{\partial(DW^2)}{\partial z} = DB - C_D W^2\,, \tag{5b}$$

$$\frac{\partial(DWB)}{\partial z} = mB\,. \tag{5c}$$

This is now a system of three oridinary differential equations in terms of unknowns W, B, D, m and empirically-derived coefficients for skin friction (C_d) and entrainment (α). If m is known a priori, then this can be integrated numerically. However, since m is the wall-source volume flux per unit area, which includes subglacial discharge (at $z = 0$) and melt rate, this can also be treated as an unknown by adding a fourth equation (either temperature or salinity) or replacing the buoyancy equation with the following equations

$$\frac{\partial(DWT)}{\partial z} = \alpha W T_a + m T_{\text{ef}}\,, \tag{6a}$$

$$\frac{\partial(DWS)}{\partial z} = \alpha W S_a + m S_i\,. \tag{6b}$$

which can be derived analogously to Eqs. (2c) and (3c) for temperature and salinity. Here, T_a and S_a are the ambient temperature and salinity. S_i is the ice interface salinity, and T_{ef} is the effective temperature gradient including latent heat, $T_{\text{ef}} = -c_w^{-1}(L_i + c_i(T_b - T_i))$, where T_b is the bulk boundary layer temperature close to the ice, and T_i is the ice interface temperature. In the context of LeConte glacier, we assume a strongly melting regime (see e.g., Wells and Worster (2008)), so the temperature of the interface is the local freezing temperature, and the interface salinity is assumed to be zero.

:

To solve for the boundary layer temperature and salinity, and melt rate, we use the three-equation thermodynamics (Hellmer & Olbers, 1989; Holland & Jenkins, 1999), which describes the thermodynamical equilibrium at the ice-ocean interface. This equilibrium can be expressed using approximate heat and salt conservation and the linearized freezing temperature of seawater,

$$m\rho_i(L + c_i(T_b - T_i)) = \rho_w \gamma_T c_w(T - T_b) \tag{7a}$$

$$m\rho_i(S_b - S_i) = \rho_w \gamma_S(S - S_b)\,, \tag{7b}$$

$$T_b = \lambda_1 S_b + \lambda_2 + \lambda_3 z\,, \tag{7c}$$

where ρ_i and ρ_w are the ice and seawater density, respectively, L, c_w, c_i are defined in Section 2, S_p is the plume salinity, S_b is the boundary layer salinity, γ_T and γ_S are the turbulent heat and salt transfer coefficients, respectively, and $\lambda_1 = -5.73 \times 10^{-2}$ °C psu^{-1}, $\lambda_2 = 8.32 \times 10^{-2}$ °C, and $\lambda_3 = 7.61 \times 10^{-4}$ °C m^{-1} are the freezing point slope, offset, and depth. These empirical values are consistent with those used in previous studies (Sciascia et al., 2013; Cowton et al., 2015). Recent parameterizations of the turbulent transfer coefficients (Jenkins et al., 2010) express the turbulent transfer coefficients in terms of near-glacial ocean velocities as

$$\gamma_T = \Gamma_T \sqrt{C_d v^2 + C_d w^2}\,, \tag{8a}$$

$$\gamma_S = \Gamma_S \sqrt{C_d v^2 + C_d w^2}\,, \tag{8b}$$

with C_d, Γ_T, v, w as defined in Section 2, and $\Gamma_S = 6.2 \times 10^{-4}$ is the salt transfer constant. However, an alternative formulation that differentiates between the external and plume-driven shear boundary layers is presented in Section 2 of the main text.

August 8, 2023, 6:47am

S-2. Model Setup Details

The model used in the study is the Massachusetts Institute of Technology General Circulation Model (MITgcm), which is available at *mitgcm.org*. Using this model, we solve the nonhydrostatic, Boussinesq primitive equations with a 3D Smagorinsky parameterization to set eddy viscosities (Smagorinsky, 1963) and a nonlinear equation of state based on Jackett and McDougall (1995). The MITgcm model configuration is available at: *https://github.com/zhazorken/MITgcm_FJ*.

References

Cowton, T., Slater, D., Sole, A., Goldberg, D., & Nienow, P. (2015). Modeling the impact of glacial runoff on fjord circulation and submarine melt rate using a new subgrid-scale parameterization for glacial plumes. *J. Geophys. Res. Oceans*, *120*, 796–812.

Hellmer, H. H., & Olbers, D. J. (1989). A two-dimensional model for the thermohaline circulation under an ice shelf. *Antarctic Science*, *1*(4), 325–336. doi: 10.1017/ S0954102089000490

Holland, D. M., & Jenkins, A. (1999). Modeling Thermodynamic Ice-Ocean Interactions at the Base of an Ice Shelf. *J. Phys. Oceanogr.*, *29*(8), 1787–1800. doi: 10.1175/ 1520-0485(1999)029⟨1787:MTIOIA⟩2.0.CO;2

Jackett, D. R., & McDougall, T. (1995). Minimal adjustment of hydrographic profiles to achieve static stability. *J. Atmos. Ocean. Technol.*, *14*(4), 381–389.

Jackson, R. H., Nash, J. D., Kienholz, C., Sutherland, D. A., Amundson, J. M., Motyka, R. J., ... Pettit, E. (2019). Meltwater intrusions reveal mechanisms for rapid subma-

rine melt at a tidewater glacier. *Geophys. Res. Lett.*. doi: 10.1029/2019GL085335

Jenkins, A., Dutrieux, P., Jacobs, S., McPhail, S., Perrett, J., Webb, A., & White, D. (2010). Observations beneath Pine Island Glacier in West Antarctica and implications for its retreat. *Nat. Geosci.*, *3*, 468–472.

Morton, B. R., Taylor, G. I., & Turner, J. S. (1956). Turbulent gravitational convection from maintained and instantaneous sources. *Proceedings of the Royal Society of London. Series A. Mathematical and Physical Sciences*, *234*(1196), 1-23. doi: 10.1098/rspa.1956.0011

Parker, D. A., Burridge, H. C., Partridge, J. L., & Linden, P. F. (2021). Vertically distributed wall sources of buoyancy. Part 1. Unconfined. *J. Fluid Mech.*, *907*, A15. doi: doi:10.1017/jfm.2020.808

Sciascia, R., Straneo, F., Cenedese, C., & Heimbach, P. (2013). Seasonal variability of submarine melt rate and circulation in an East Greenland fjord. *J. Geophys. Res. Oceans*, *118*, 2492–2506.

Wells, A., & Worster, M. (2008). A geophysical-scale model of vertical natural convection boundary layers. , *609*, 111–137. doi: 10.1017/S0022112008002346
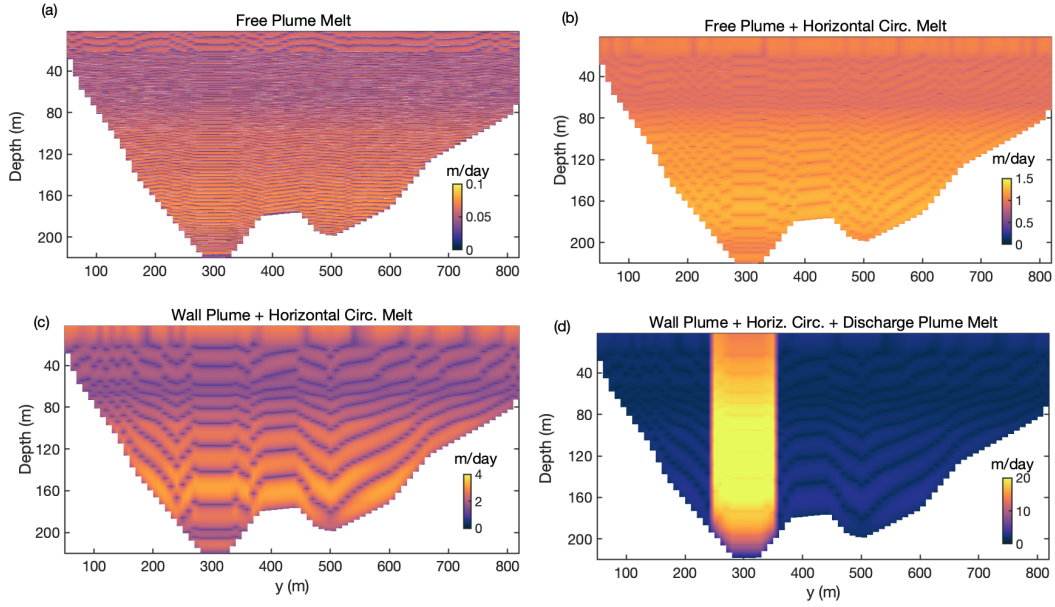
Figure S1. Melt rates at the LeConte glacier face calculated using (a) free plume parameters (Jackson et al., 2019), (b) free plume parameters with an additional horizontal circulation melt contribution driven by a uniform horizontal velocity of $v = 0.2$ m/s, (c) wall plume parameters with the same horizontal circulation melt contribution, and (d) wall plume parameters with the same horizontal circulation melt contribution and a 100-meter wide discharge plume with a discharge rate 220 m^3/s.